Archives of Materials Science and Engineering

Volume 58
Issue 2
December 2012
Pages 177-181

International Scientific Journal
published monthly by the
World Academy of Materials
and Manufacturing Engineering

Multi-variant calculations of induction heating process

A. Smalcerz [a,*] , R. Przyłucki [a], K. Konopka [b], A. Fornalczyk [c], M. Ślezok [d]

[a] Managements and Informatics Department, Faculty of Materials Engineering and Metallurgy, Silesian University of Technology, ul. Krasińskiego 8, 40-019 Katowice, Poland
[b] Institute of Measurement Science, Electronics and Control, Faculty of Electrical Engineering, Silesian University of Technology, ul. Akademicka 10, 44-100 Gliwice, Poland
[c] Metallurgy Department, Faculty of Materials Engineering and Metallurgy, Silesian University of Technology, ul. Krasińskiego 8, 40-019 Katowice, Poland
[d] University of Economics and Administration, ul. A. Frycza-Modrzewskiego 12, 41-907 Bytom, Poland
* Corresponding e-mail address: albert.smalcerz@polsl.pl

Received 29.10.2012; published in revised form 01.12.2012

ABSTRACT

Purpose: Induction heating process is often used as the first stage of quenching process. Computer simulation of the induction heating make it possible to eliminate expensive and time-consuming experimental selection of parameters. The selection of appropriate heating parameters is particularly difficult for the irregularly shaped parts. Gears are an example of such elements. In the case of surface quenching / heating a uniform distribution of temperature field is necessary on the surface and expected temperature gradient inside the heated gear. The following parameters: inductor frequency, inductor power, heating time, inductor geometry, distance between inductor and heating gear and relative shift between inductor and gear have a significant effect on the temperature distribution. Obtaining the correct temperature distribution requires proper selection of the above mentioned parameters. Numerical optimization or multi-variant calculations are the best way to achieve the goal.

Design/methodology/approach: This work presents numerical simulation of induction heating. Such simulation consists of an analysis of coupled electromagnetic and thermal fields. Commercial program Flux 3D, was used to perform the calculations.

Findings: Execution of 10 variants of calculation enables to obtain the optimal values of the parameters influencing the heating process.

Practical implications: During the test quenching of the gear a problem of non uniform temperature distribution appears. The attempts of experimental selection of heating parameters failed, and the problem was solved by multi-variant calculations. The results obtained from the calculations were successfully applied in the quenching process.

Originality/value: This paper shows an application of numerical simulation in gear quenching. The results of simulations were practically verified.

Keywords: Induction heating; Quenching; Coupled electromagnetic-thermal calculation; Temperature measurement verification; Gears

Reference to this paper should be given in the following way:

A. Smalcerz, R. Przyłucki, K. Konopka, A. Fornalczyk, M. Ślezok, Multi-variant calculations of induction heating process, Archives of Materials Science and Engineering 58/2 (2012) 177-181.

METHODOLOGY OF RESEARCH, ANALYSIS AND MODELLING

1. Introduction

Quenching is a popular method that can be used to improve mechanical properties of steel. Quenching process consists of two stages: heating (over the austenitizing temperature) and fast cooling [1,2,3]. Depending on the applications, either volume or surface quenching is used. In the case of surface quenching it is very important to heat only the surface layer of the work-piece, and temperature distribution on the surface layer should be uniform. For irregularly shaped parts, for example gears, it is very difficult to obtain a uniform surface temperature distribution [4,5]. The most popular technique used in surface heating is induction heating. Its main advantage is the possibility of achieving high volumetric power density. This method is dedicated to surface heating because power is dissipated directly in the heated charge only in the outside layer of the work-piece (skin effect) [6,7]. The depth of field penetration depends on the inductor's frequency.

In this article the simulation of surface induction heating process of gear is presented. Small gears (Fig. 1) are usually heated in a cylindrical inductor. A large number of parameters influence the temperature distribution in the heated element. The main of them are:

- gear material properties;
- inductor current frequency;
- inductor power;
- heating time;
- inductor geometry (number of coils, diameter of coil, geometry of coil profile);
- vertical displacement between coil and gear (Fig. 3).

In some cases, during the heating process, gear slowly rotates in inductor for the temperature equalization. If it is necessary heating with use of pulsing dual-frequency is used [8,9,10,11].

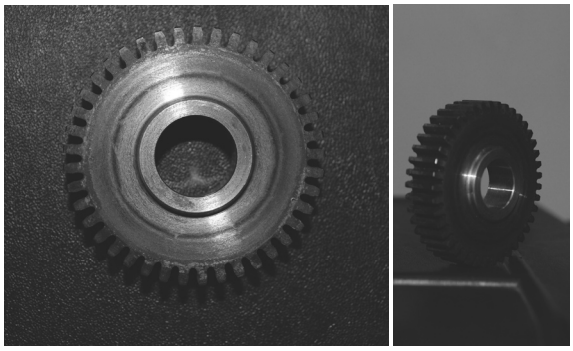

Fig. 1. Real view of gear

The aim of this work was an appropriate choice of three parameters of the heating process: heating power (voltage), vertical shift between inductor and coil, and time. During the experiment temperature value and distribution on the surface of the gear were monitored. Temperature distribution in the gear cross-section on six paths was monitored, too.

The parameters determined in the experiment were used in a real quenching stand and temperature distribution was verified with the IR camera.

2. Research description and calculation model

Surface quenching of the gear is not a simple issue. One of the difficulties is to obtain the temperature range above austenitizing (in the considered case 1100°C). The second obtain a uniform temperature distribution on essential surfaces of gear. Uniform distribution of temperature should be obtained on the tooth and notch surfaces (Fig. 4), while the deeper layers should remain in the lower temperature (below 750°C).

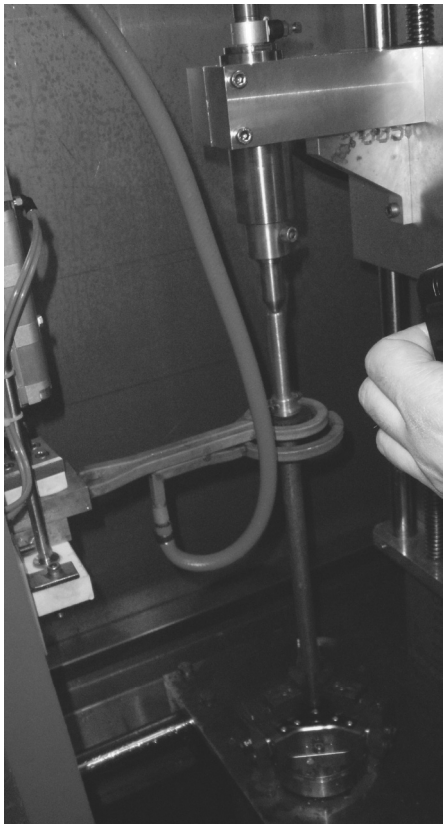

Fig. 2. Real view of quenching stand

Quenching stand considered in this article is shown in Fig. 2. It consists of inductor, heated gear and gear gripping system. The cross section of the heating / quenching system is presented in Fig. 3, and the sketch of the gear in Fig. 4. The main dimensions of the system are: gear radius rg = 16 mm (Fig. 3), gear hole diameter Φ_1 = 13.9 mm (Fig. 4), gear height g_h = 13.7 mm, inductors height i_h = 10 mm, offset between inductor and gear h (Fig. 3) was changed in each considered variant.

The gear were made of alloy steel - EN 10083-1, gear gripping system from brass and the inductor was made from copper. The calculation model was limited to one tooth due to the periodicity of the system. The view of calculation model is presented in Fig. 5. Material properties used in calculation model are presented in Table 1 [12,13,14].

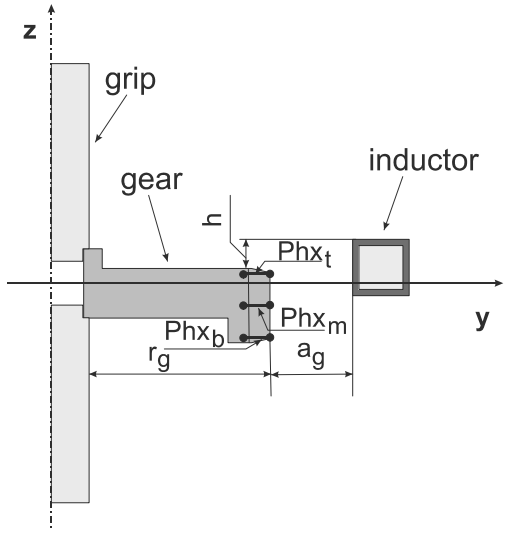

Fig. 3. Quenching stand - cross section

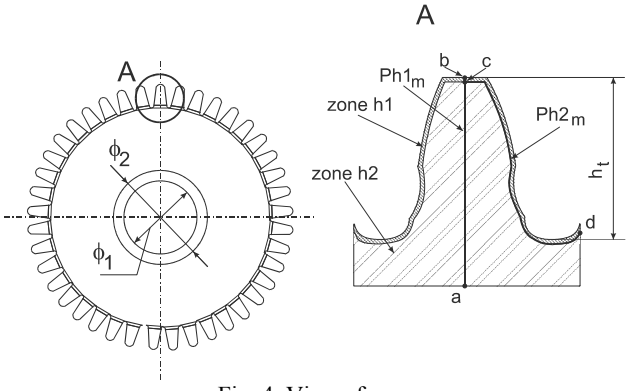

Fig. 4. View of gear

Table 1.
Material properties

Property	Kind of approximation	Approximation parameters
Steel rho, Ωm	Linear $\rho = \rho_0(1+aT)$	$\rho_0 = 2.5\cdot10^{-7}$ Ωm, a = 0.004 (°C)$^{-}$
Brass rho, Ωm	-	$\rho = 0.4\cdot10^{-7}$ Ωm
Copper rho, Ωm	-	$\rho = 1.8\cdot10^{-8}$ Ωm
Steel μ_r,	special function [1]	μ(0°C)=10
Brass, Cooper μ_r,	-	1
Steel λ, W/mK	Linear $\lambda = \lambda_0(1+aT)$	$\rho_0 = 47$ W/mK, a = -0.0025 (°C)$^{-}$
Steel γc, J/(m^{3}K)	special function [2]	γc(0°C)=4·10^6

[1] Special fuction 1:

$$B(H) = J_S \frac{H_a + 1 - \sqrt{(H_a+1)^2 - 4H_a(1-a)}}{2(1-a)} + \mu_0 H; \quad H_a = \mu_0 H \frac{(\mu_{r0}-1)}{J_S}$$

[2] Special fuction 2:

$$\rho c = \frac{E}{\sigma\sqrt{2\pi}} e^{\left(\frac{T-T_c}{\sigma}\right)} + (V_0 - V_i) e^{-\frac{T}{\tau}} + V_i$$

During the experiment 10 calculation variants were considered. The variants differ in: offset between inductor and gear and inductor power. The power was controlled by changing the inductor current. The calculations were conducted until the maximum temperature in the heated gear reached 1100°C. All calculation variants' parameters are included in Table 2.

Table 2
Calculation variants

Variant	Inductor's current A	Inductor - gear shift mm
v1	2 300	-5
v2	2 300	0
v3	2 300	5
v4	2 400	-5
v5	2 400	0
v6	2 400	5
v7	2 500	-5
v8	2 500	0
v9	2 500	5
v10	2 419	?

The calculations were carried out with the use of Flux 3D program. It is a commercial program allowing to conduct three dimensional, coupled analysis of the electromagnetic and thermal fields. The program uses the finite element method.

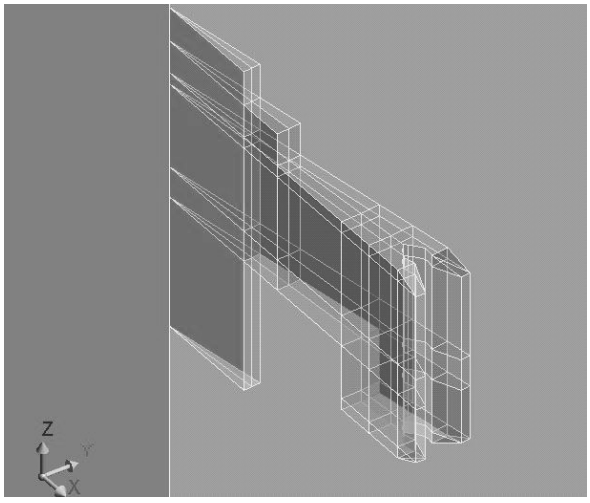

Fig. 5. Calculation model

The calculations of the electromagnetic field, due to the periodicity of the system, were limited to 1 tooth with cyclic boundary condition adopted for the respective edges (Fig. 5). For the induction heating electromagnetic field is described in symbolic form (steady state problem). Four different formulations of state variable of electromagnetic field are implemented in the calculation program: AV-A, TΦ-Φ-$\Phi_{red.}$, TΦ-Φ-$\Phi_{red.T0}$, AV - Φ or $\Phi_{red.}$. The formulations differ in the precision of calculation, acceptable model geometries and number of state variables required to describe the EM field. In the calculations, except current density **J** and magnetic field intensity **H**, pair of potentials

T and Φ is used [15]. For massive conductors (gear, grip) the pair of equations (1), (2) is used. For the inductor, modeled as stranded coil, equation (3) is used. For the air surrounding the calculation model, equation (4) is used.

$$\boldsymbol{J}=\nabla\times\boldsymbol{T} \tag{1}$$

$$\boldsymbol{H}=\boldsymbol{T}-\nabla\boldsymbol{\Phi} \tag{2}$$

$$\boldsymbol{H}=\boldsymbol{T}_0-\nabla\boldsymbol{\Phi}_{red.T0} \tag{3}$$

$$\boldsymbol{H}=\boldsymbol{H}_j-\nabla\boldsymbol{\Phi} \tag{4}$$

where:
J - eddy current density;
T - vector potential of electric field;
T_0 - source electric vector potential generated by the non meshed coil;
Φ - scalar potential of magnetic;
$F_{red.\ T0}$ - reduced scalar potential with respect to T0;
H - magnetic field intensity,
H_j - magnetic field intensity calculated according to Biot-Savart law.

The computational model was surrounded by the external element "infinity" that models an area wide enough to decay of the electromagnetic field on its outside edges.

Thermal field analysis was limited to the gear area only. The calculations were carried out based on the equation (5). On the outside edges of the gear, boundary condition (6) was adopted.

$$\nabla\cdot\left(-\lambda\nabla T\right)+\rho c\frac{\partial T}{\partial t}=q \tag{5}$$

$$-\lambda\frac{\partial T}{\partial n_P}=\alpha(T-T_o)+\varepsilon\sigma(T^4-T_o^4) \tag{6}$$

where:
λ - thermal conductivity;
T - temperature;
T_0 - ambient temperature;
α - heat transfer coefficient;
ε - emissivity;
σ - Stefana-Boltzman constat.

3. Experiment results

During the experiment the maximum temperature and temperature distribution along six paths were monitored. Location of the two paths ($ph1_m$ and $ph2_m$) is shown in Fig. 4. These paths are located in the middle of the gear's tooth *z* dimension (Fig. 3). Other paths are located 0.26 mm from top and bottom edges of the gear and have indexes *t* and *b*, respectively. On Figure 6 temperature distribution along path Ph1m dependant on inductor shift h are presented. Gear was surface heated, after three seconds of heating zone h1 (Fig. 3) was about 2.6 mm for variant v5.

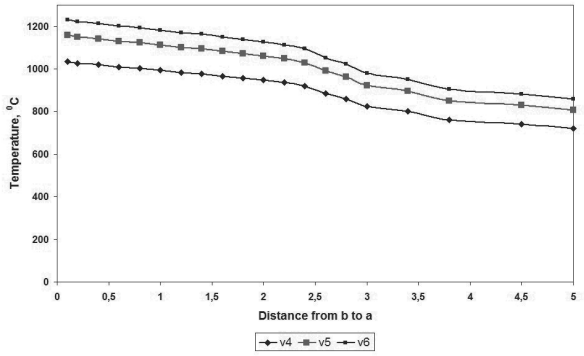

Fig. 6. Dependency of temperature distribution along path Ph1m on inductor shift (h) (inductor current I = 2 400 A)

On Figure 7 temperature distribution along path Ph2b dependant on inductor shift h are presented. After three seconds of heating proper temperature distribution was obtained only for variant v10. For other variants temperature was to high (v3) or too low (v1). Similar results were obtained for paths Ph2m and Ph2t.

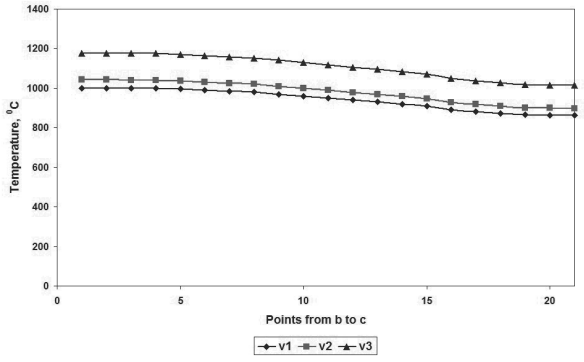

Fig. 7. Dependency of temperature distribution along path ph2b on inductor shift (h) (inductor current I = 2 300)

Figure 8 shows dependency of temperature distribution on the path Ph2t on the inductor current. As might be expected increase of current causes increase of temperature. Proper temperature regime is obtained for variant v5 only.

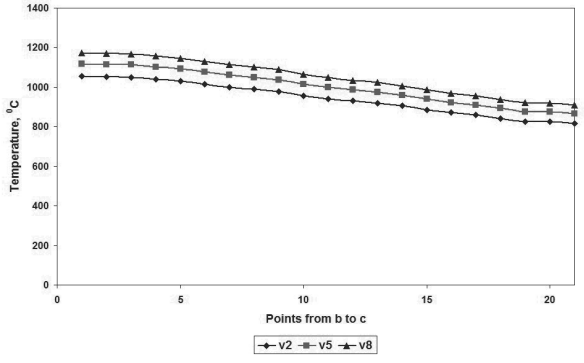

Fig. 8. Dependency of temperature distribution along path Ph2t on the inductor current (h=0)

The results most similar to the expected were obtained for the variant v10. For this variant shift between inductor and gear h = -0.9 mm, (current I = 2 419 A). For such selected parameters real quenching process was carried out. During the heating temperature of surface of gear was controlled by IR camera. On the Figures 9 and 10 temperature distribution from simulation and real heating process are presented.

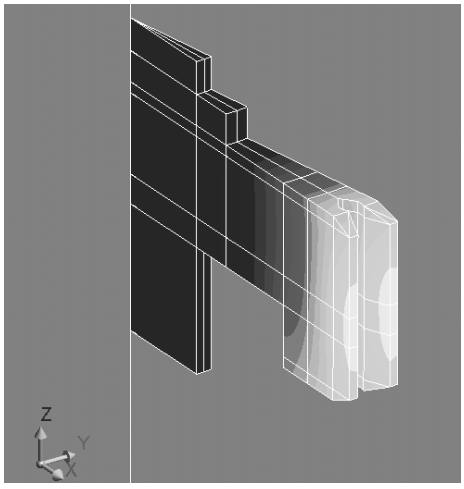

Fig. 9. Temperature distribution from simulation (after 3 sec of heating)

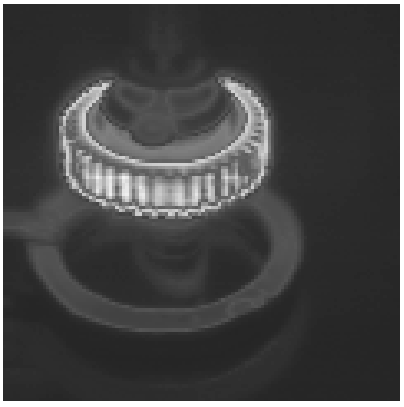

Fig. 10. IR camera image of temperature distribution of heating gear (after 3 sec of heating)

4. Conclusions

This work presents numerical simulation of induction heating. Such simulation consists of an analysis of coupled electromagnetic and thermal fields. During the test quenching of the gear a problem of non uniform temperature distribution appears. The attempts of experimental selection of heating parameters failed, and the problem was solved by multi-variant calculations. The results obtained from the calculations were successfully applied in the quenching process. Execution of 10 variants of calculation enables to obtain the optimal values of the parameters influencing the heating process. During the experiment 10 calculation variants were considered. The variants differ in: offset between inductor and gear and inductor power. The results most similar to the expected were obtained for the variant v 10. For this variant shift between inductor and gear h = -0 9 mm, (current 2 419 A). Real quenching process were done for such parameters and temperature distribution on the gear surface after heating were verified with temperature distribution obtained from calculation (Fig. 10. and Fig. 9. respectively).

For these heating parameters expected values and zones of quenching were obtained.

Acknowledgements

Financial support from Polish Ministry of Science and Higher Education is acknowledged (contract No N N508 479438).

References

[1] V. Rudnev, D. Loveless, R. Cook, M. Black, Induction hardening of gears, a review, Heat Treatment of Metals 4 (2003) 97-103.
[2] V. Rudnev, Induction hardening of gears, a review, Part 1, Heat Treatment of Metals, Wolfson Heat Treatment Centre, England, 2003, 97-103.
[3] V. Rudnev, et al., Induction hardening of gears, a review, Part 2, Heat Treatment of Metals, Wolfson Heat Treatment Centre, 2004, 11-15.
[4] G. Parris, D. Ingham, The submerged induction hardening of gears, Gear Technology, 2001, 28-40.
[5] V. Rudnev, Systematic analysis of induction coil failures, Part 5, Effect of flux concentrators on coil life, Heat Treating Progress, 2006, 21-26.
[6] M. Fisk, Simulation of induction heating in manufacturing, Licentiate Thesis, 2008.
[7] R. Przyłucki, Calculations of the induction heating system with the monitoring of thermal stress in charge, Electrical Review 11 (2008) 210-214.
[8] S. Lupi, F. Doughiero, M. Forzan, Modelling single- and double-frequency induction hardening of gear-wheels, Proceedings of the Conference EPM'2006, Sendai, 2006, 473-478.
[9] M. Niklewicz, A. Smalcerz, The use of three-coil cylindrical inductor in the gear induction heating process, Electrical Review 5 (2010) 333-335 (in Polish).
[10] J. Barglik, A. Kurek, D. Dołęga, et al., Induction hardening of gear wheels - numerical simulation, Proceedings of the 10th International Scientific Conference EPE, Czech Republic, 2009.
[11] M. Niklewicz, A. Smalcerz, A. Kurek, Estimation of system geometry and inductor frequency importance in induction hardening process of gears, Electrical Review 11 (2008) 219-224.
[12] J.R. Davis, Gear materials, properties and manufacture, ASM International, 2005.
[13] Materials base: www.matweb.com.
[14] Materials base: www.knovel.com/knovel2/default.jsp.
[15] Flux3D v.9.1 User's guide 2004.